2mu4

NASA TECHNICAL NOTE

NASA TN D-7675

NASA TN D-7675

TECHNIQUE FOR DIRECT MEASUREMENT OF MAGNETIC ENTROPY OF SOLIDS - RESULTS FOR DYSPROSIUM TITANIUM OXIDE

by Dennis J. Flood

Lewis Research Center
Cleveland, Ohio 44135

NATIONAL AERONAUTICS AND SPACE ADMINISTRATION • WASHINGTON, D. C. • MAY 1974

1. Report No.	2. Government Accession No.	3. Recipient's Catalog No.
NASA TN D-7675		

4. Title and Subtitle	5. Report Date
TECHNIQUE FOR DIRECT MEASUREMENT OF MAGNETIC ENTROPY OF SOLIDS - RESULTS FOR DYSPROSIUM TITANIUM OXIDE	May 1974
	6. Performing Organization Code
7. Author(s)	8. Performing Organization Report No.
Dennis J. Flood	E-7859
	10. Work Unit No.
9. Performing Organization Name and Address	502-10
Lewis Research Center National Aeronautics and Space Administration Cleveland, Ohio 44135	11. Contract or Grant No.
	13. Type of Report and Period Covered
12. Sponsoring Agency Name and Address	Technical Note
National Aeronautics and Space Administration Washington, D.C. 20546	14. Sponsoring Agency Code

15. Supplementary Notes

16. Abstract

A measurement technique was devised which permits direct observation of the magnetic entropy of solids as a function of applied magnetic field. Measurements were made of the magnetic entropy, in the temperature range 2 to 20 K, of polycrystalline samples of dysprosium titanium oxide ($Dy_2Ti_2O_7$) to determine its suitability for use as the working substance of a magnetic refrigerator. Magnetization measurements were also made at 4.2 K and below to provide additional information on the nature of the compound. The measurements indicated that crystalline electric fields perturbed the ground state of the dysprosium^{+++} ions, removed the 16-fold degeneracy predicted by Hund's rules, and left only a twofold degeneracy in its place. A positive, temperature independent contribution to the magnetization was observed in the saturation region, which indicated that the doublet ground-state wave function was perturbed by a nearby unpopulated upper energy level. The lowest energy level was, however, very nearly a pure $J_z = \pm 15/2$ state, with $n_B = 9.4 \pm 0.4$ Bohr magnetons per ion, where J_z is the z-component of total angular momentum, and n_B is the number of Bohr magnetons per ion ($n_B = 10$ for a pure $\pm 15/2$ state). The isothermal changes in magnetic entropy as a function of applied field were combined with adiabatic demagnetization temperature measurements to plot the constant-field lines in the entropy-temperature plane. The data indicated that a practical magnetic refrigeration cycle could be operated between 4.2 and 20 K and that $Dy_2Ti_2O_7$ has a maximum cooling capacity, with a 10-T maximum applied field, of 31 J/kg.

17. Key Words (Suggested by Author(s))		18. Distribution Statement
Magnetization	Magnetic insulators	Unclassified - unlimited
Magnetic entropy	Solids	Category 18

19. Security Classif. (of this report)	20. Security Classif. (of this page)	21. No. of Pages	22. Price*
Unclassified	Unclassified	26	$3.00

* For sale by the National Technical Information Service, Springfield, Virginia 22151

TECHNIQUE FOR DIRECT MEASUREMENT OF MAGNETIC ENTROPY OF SOLIDS - RESULTS FOR DYSPROSIUM TITANIUM OXIDE

by Dennis J. Flood

Lewis Research Center

SUMMARY

A measurement technique was devised which permits direct observation of the magnetic entropy of solids as a function of applied magnetic field. Measurements were made of the magnetic entropy, in the temperature range 2 to 20 K, of polycrystalline samples of dysprosium titanium oxide ($Dy_2Ti_2O_7$) to determine its suitability for use as the working substance of a magnetic refrigerator. Magnetization measurements were also made at 4.2 K and below to provide additional information on the nature of the compound. The measurements indicated that crystalline electric fields perturbed the ground state of the dysprosium^{+++} ions, removed the 16-fold degeneracy predicted by Hund's rules, and left only a twofold degeneracy in its place. A positive, temperature independent contribution to the magnetization was observed in the saturation region, which indicated that the doublet ground-state wave function was perturbed by a nearby unpopulated upper energy level. The lowest energy level was, however, very nearly a pure $J_z = \pm 15/2$ state, with $n_B = 9.4 \pm 0.4$ Bohr magnetons per ion, where J_z is the z-component of total angular momentum and n_B is the number of Bohr magnetons per ion ($n_B = 10$ for a pure $\pm 15/2$ state).

The isothermal changes in magnetic entropy as a function of applied field were combined with adiabatic demagnetization temperature measurements to plot the constant-field lines in the entropy-temperature plane. The data indicated that a practical magnetic refrigeration cycle could be operated between 4.2 and 20 K and that $Dy_2Ti_2O_7$ has a maximum cooling capacity, with a 10-tesla maximum applied field, of 31 joules per kilogram.

INTRODUCTION

The development of a magnetic refrigerator for operation at temperatures above 4.2 K, for example, between boiling liquid helium and boiling liquid hydrogen (refs. 1

and 2), can be greatly facilitated by knowledge of the temperature and field dependence of the magnetic entropy of the paramagnetic working substance. Such information has usually been obtained indirectly by measuring the total specific heat of the material, separating the magnetic from the nonmagnetic contributions, and then computing the entropy from the appropriate thermodynamic relations. The analysis involves a great deal of computation, either for curve fitting, for example, or for numerical integration. The experimental procedure to be discussed in this report permits direct observation of changes in the magnetic entropy of solids as a function of magnetic field. The need for involved calculations to obtain the entropy values is completely circumvented.

The technique was used to measure the isothermal changes in magnetic entropy, as a function of magnetic field, for the compound dysprosium titanium oxide ($Dy_2Ti_2O_7$). These data, coupled with adiabatic magnetization-demagnetization measurements, were used to map the isofield lines in the magnetic-entropy - temperature plane. Furthermore, the absolute values of magnetic entropy, not just relative changes, were determined. The latter was possible because at temperatures below 4.2 K the magnetic entropy of the sample was reduced essentially to zero in a 10-tesla magnetic field.

The magnetization of the compound was also studied as a function of applied magnetic field for several temperatures in the liquid-helium range. The results were useful, as supplementary information to the magnetic entropy measurements, for obtaining a more complete understanding of the magnetic properties of $Dy_2Ti_2O_7$.

EXPERIMENT

Sample Preparation

The compound was obtained from a commercial supplier in powder form. An X-ray analysis performed on the sample as received yielded a powder pattern in agreement with that published by Roth (ref. 3). A portion of the sample which had been compressed at approximately 5000 atmospheres into a solid cylinder was heated in air at 1200° C for about 8 hours. The solid rod which was produced had a density of 5 grams per cubic centimeter. A section of the rod was cut off and shaped approximately like an ellipsoid of revolution (major axis, 1.02 cm; minor axis, 0.413 cm) for the magnetic-entropy measurements. A part of the untreated powder which was left was used for the magnetization measurements.

Apparatus

Two magnets were used for these experiments. One was a conventional supercon-

ductive solenoid capable of generating 10.4 teslas in a 6.35-centimeter-diameter bore. The second was a water-cooled, 10.16-centimeter-diameter-bore solenoid which could produce a peak field of approximately 8 teslas (ref. 4) and could be brought to full field in times varying from a few seconds to several minutes.

Figure 1 is a sketch of the apparatus used for the magnetic entropy measurements. The sample was clamped between two phenolic disks which were held together by three number 4 nylon screws. The clamp assembly was suspended from a third phenolic disk by means of a single, hollow, number 10 stainless-steel screw, and the whole assembly was in turn suspended with three number 4 nylon screws from the bottom of a copper heat sink. This arrangement provided satisfactory thermal isolation from the heat sink and was strong enough to allow the apparatus to be removed, if necessary, from the magnet when a relatively high field was present. (The saturation magnetization of the sample is nearly one-fourth that of iron, so that large forces are exerted on it as it is pulled through a region of high field gradient.)

Since the magnetic-entropy measurements were made at fixed temperature, no particular concern had to be given to extraneous heat capacities. The adiabatic measurements, however, required that all such heat capacities be minimized, or at least carefully determined. Figure 2 shows the sample holder which was constructed for these measurements. The sample was suspended from a clear plastic framework by nylon thread, with only a carbon thermometer glued to a small strip of copper attached to it. Short lengths of resistance wire were inserted between the thermometer leads and the electrical leads of the cryostat to reduce thermal conduction. The thermal stability achieved by this mounting technique was such that no appreciable temperature drift occurred during the course of a magnetization-demagnetization cycle.

Magnetization measurements were made by using the apparatus shown in figure 3. The two hollow phenolic cylinders were each wound with 750-turn pickup coils. The cylinders were suspended in the magnet in a side-by-side arrangement to take advantage of the homogeneity of the field in the central region of the water-cooled solenoid. This arrangement permitted the use of samples with length-diameter ratios great enough ($\sim$ 10:1) that demagnetizing effects at the location of the pickup coil were negligible. At the same time, the sample diameters were sufficiently large that the voltages generated were easily detected. The sample length was 7.58 centimeters, and its diameter was 0.71 centimeter. The mean area of each pickup coil was 0.72 square centimeter.

Measurement Techniques

Figure 4 illustrates how the magnetic entropy measurements were made. A heater was noninductively wound on the sample, glued securely to it with adhesive varnish, and connected to a temperature controller. The sensing element for the controller was a

glass-ceramic capacitor (refs. 5 and 6). The controller was a commercially available unit consisting of a capacitance bridge and a feedback network for regulating heater power. The supplier of the thermometer and controller also provided a certified temperature calibration of the unit from 1.5 to 300 K. Calibration points below 1.5 K were obtained by direct comparison with helium vapor pressure measurements. The capacitor was glued to a strip of 0.005-centimeter-thick copper foil which was in turn glued to the sample. The foil was wrapped around both the sample and the thermometer and was trimmed so that its ends did not quite meet. Signals proportional to the heater voltage and current were used as inputs to a multiplier. The multiplier output, which was proportional to the power supplied to the heater, was applied to the input of an integrator.

At constant temperature,

$$\int \left(\frac{dQ}{dt}\right) dt = \Delta Q = T\Delta S \tag{1}$$

where ΔQ is the heat supplied by the heater, T is the absolute temperature, and S is the entropy. Hence, the integrator output was proportional to ΔS, the change in entropy of the sample. (Symbols are defined in appendix A.) Keeping the temperature constant while varying the magnetic field means that only the magnetic entropy can change. The entropy of the crystalline lattice, thermometers, and so on should be unaffected if they are nonmagnetic. A precision 10-turn potentiometer was inserted between the integrator and the X, Y-plotter to divide the signal by a factor proportional to the temperature.

Data were taken after first establishing a steady-state temperature for the sample by balancing heater output against the heat lost from thermal conduction to the helium bath. It was intended that most of the heat be conducted to the bath by helium gas which had been admitted to the vacuum chamber, although a small fraction of it was carried by the electrical leads to the heat sink. The helium gas pressure was typically 100 millitorr. In order to avoid integrating the steady-state heater power background, a bucking voltage equal in magnitude to the multiplier output was also applied to the integrator prior to changing the magnetic field. Hence, only the change in heater power caused by the change in magnetization as a function of applied field was integrated. A systematic error was introduced into the measurements nonetheless by the slight magnetoresistance of the heater wire and the thermal magnetoresistance of the leads. The two effects caused the power required to maintain a steady temperature to vary with magnetic field. To correct for the error thus introduced into the measurements, the steady-state power required to maintain a particular temperature was determined for several values of magnetic field. The variation in required power was nearly linear in magnetic field in all cases so that an analytical expression could be developed to correct the data. (See

appendix B for a more complete discussion.) It was also possible, by manually readjusting the steady-state bucking voltage, to correct the measurements as they were made. Since the latter procedure was extremely tedious, it was used only a few times to verify the corrections made analytically. The two methods gave results which agreed with one another to within ±5 percent. The principal contribution to the uncertainty of the results, aside from the approximations made in estimating the correction term mentioned previously, was integrator drift. Measurement errors associated with the rest of the instrumentation were generally 1 percent or less.

Figure 5 shows the method used to detect changes in sample temperature during the adiabatic magnetization-demagnetization experiments. The sample was mounted in the sample holder shown in figure 2, but without the heater wrapped on it. The capacitance thermometer was replaced by a calibrated carbon resistor so that data could be taken continuously as a function of applied field. The measurements were made as follows: Thermometer resistance as a function of time was first recorded to determine temperature drift rates. Then thermometer resistance was recorded parametrically as a function of magnetic field with time as the parameter. Finally, when temperature drift was determined to be negligible over the time of the measurement, thermometer resistance was plotted directly as a function of magnetic field. The thermometer current was typically 1 microampere, so that heating caused by power dissipation in the resistor could be neglected.

Figure 6 shows the way in which magnetization measurements were made. The sample was packed to an average density of 3.86 grams per cubic centimeter into one of the phenolic cylinders, and the pickup coils were connected to the integrator input in opposition to one another. The integral of the voltage difference between the two coils was proportional to the magnetization of the sample and was recorded by the X, Y-plotter as a function of field. A slight mismatch between the coils produced a nonzero difference voltage when both were empty. This condition resulted in the superposition of a linear background on the integrator output. The slope of the background was easily determined, however, and the data were corrected accordingly.

The phenolic cylinders were immersed in liquid helium for the measurements, and field sweeps were made slowly enough so that thermal equilibrium was maintained throughout the sample. A suitable rate was determined by changing the current in the magnet at various speeds until no differences were discernible in the magnetization traces while the field was increased or decreased.

RESULTS AND DISCUSSION

The isothermal traces of magnetic entropy changes as a function of magnetic field are shown in figure 7 for several temperatures. The curves show quite clearly the

close approach to zero entropy at the lower temperatures by the time the applied magnetic field has reached 10 teslas. Magnetic entropy changes at higher temperatures have been placed in their proper locations in the S, H-plane by using the curve shown in figure 8. Here is shown a plot of sample temperatures, measured while adiabatically magnetizing and demagnetizing the sample, as a function of applied field. The value of magnetic entropy at the higher temperature and field can be determined by starting at a temperature for which the absolute value of magnetic entropy is known and correcting for the entropy absorbed by the lattice. The isotherm for the entropy change at that temperature is then simply shifted in the S, H-plane to pass through those coordinates. The correction for the lattice entropy is given by the well-known expression

$$S_l = \frac{1}{3} aT^3 \tag{2}$$

for temperatures well below θ_D, the Debye constant for the material in question. The value of a used was that reported by van Geuns (ref. 2), namely, 2.2×10^{-6} joules per gram per kelvin. Because the mass of the thermometer was so small compared to that of the sample, no further corrections were made. Equation (2) is a good approximation even at 20 K, the entropy differing from that calculated by using the Debye function by an amount less than the 5-percent uncertainty associated with the entropy measurements themselves.

The theoretically expected maximum value for the magnetic entropy of $Dy_2Ti_2O_7$ is given by (see, e.g., ref. 7)

$$S_m = \frac{2N_o k}{M} \ln (2J + 1)$$

$$= 0.0864 \text{ J/(g)(K)} \tag{3}$$

where N_o is Avogadro's number; M is the gram-molecular weight; k is Boltzmann's constant; and J is the total angular momentum quantum number, equal to 15/2 for the ground state of the free dysprosium^{+++} (Dy^{+++}) ion. As can be seen in figure 7, however, the entropy in zero field falls far short of the value in equation (3). The results are, in fact, more consistent with a ground state degeneracy of 2, since in that case $S_m = 0.0216$ joule per gram per kelvin. Although the maximum entropy indicated in figure 7 is about 8 percent below even the latter value, it is sufficiently close to warrant the conclusion that the free-ion 16-fold ground state degeneracy has been removed by crystalline field interactions and instead only a twofold degeneracy has been left.

This conclusion is further substantiated by the magnetization measurements, the results of which are shown in figure 9. The presence of a linear magnetization, independent of temperature, is clearly evident in the saturation region. A contribution of this sort to M is a result of a perturbation of the ground state wave function of the system by nearby upper energy levels and is known as van Vleck paramagnetism (ref. 8). The separation between energy levels with differing J values is large enough in the $L \cdot S$ coupling scheme, which works well for the rare-earth ions (ref. 9), that only the lowest-lying multiplet need be considered. All others remain unpopulated at ordinary temperatures, for example, room temperature and below. Perturbation of the ground state multiplet by crystalline electric fields removes the original degeneracy and can result in a spacing of the levels which is favorable for van Vleck paramagnetism. Accordingly, the saturation magnetization is given by

$$M_S = Ng_p J' \mu_B + \alpha(H) \tag{4}$$

where N is the number of ions per cubic centimeter; g_p is the spectroscopic splitting factor appropriate for, in this case, a powdered sample; J' is the effective spin of the ground state; μ_B is the Bohr magneton; and $\alpha(H)$ is the van Vleck contribution. Crystal field calculations for the magnetically dilute compound $Dy_{0.2}Y_{1.8}Ti_2O_7$ by Townsend and Crossley (ref. 10) indicate that the ground state wave function of the Dy^{+++} ion is almost a pure J_z $\pm 15/2$ doubly degenerate state. In such a case $J' = 1/2$ and $g_\perp = 0$, while

$$g_p \equiv g_{||} = 2\langle J \rangle g_L \tag{5}$$

The quantity $g_\perp$ is the splitting factor for the plane perpendicular to the "easy direction" of magnetization, $g_{||}$ is the splitting factor parallel to the easy direction, and g_L is the free-ion Landé splitting factor. The average projection along a specified direction of N randomly oriented vectors (i.e., the "easy direction" of a crystallite) is just

$$N_{||} = \frac{2N}{4\pi} \int_0^{\pi/2} \int_0^{2\pi} \cos\theta \sin\theta \, d\theta \, d\varphi$$

$$= \frac{N}{2} \tag{6}$$

Hence, the number of Bohr magnetons per ion, based on this result, is given by

$$n_B = g_p J' = \frac{2M_s}{N\mu_B} \tag{7}$$

Extrapolating from the saturation region back to $H = 0$ in figure 9 yields $M_s = (3.79 \pm 0.08) \times 10^5$ amperes per meter (4.76 ± 0.1 kG). The ionic density of the sample used was 9.7×10^{21} ions per cubic centimeter, so that $n_B = 9.4 \pm 0.2$, which gives $g_{||} = 18.8 \pm 0.4$. The free-ion Landé g-factor is 4/3, so that equation (5) gives $g_{||} = 20$. The difference between the two values arises from the fact that the ground state wave function in reality does contain an admixture of terms and that the magnetization does have components along other directions as well. The additional terms contribute only slightly, however, as evidenced by the close agreement between the experimental and calculated values for $g_{||}$ and by the smallness of the observed van Vleck paramagnetism. The essential point is that the magnetization results are consistent with a doubly degenerate, highly anisotropic ground state.

The importance of the high-field magnetization measurements for clarifying the nature of the magnetic energy levels of the compound can be demonstrated by considering figure 10. The slope of the curve of $1/\chi$ plotted against T at low field gives the Curie constant C in the expression

$$\chi = \frac{C}{T + \Theta} \tag{8}$$

and C is given by (ref. 9)

$$C = \frac{Np_{eff}^2 \mu_B^2}{3k} \tag{9}$$

where $p_{eff} = g\sqrt{J(J+1)} = 10.63$ for the free Dy^{+++} ion. From the figure $C = 0.168 \pm 0.004$, so that from equation (9) $p_{eff} = 9.6 \pm 0.2$, a value in fairly close agreement with the free-ion value. Since the temperature at which the measurements were made is fairly close to the Neél temperature, it is reasonable to assume that magnetic interactions between the Dy^{+++} ions are beginning to become important. In that case equation (8) is no longer quite appropriate, so that deviations from the free-ion value might occur. It might then be concluded that the compound has an isotropic g-factor ($g_p^2 = 1/3(g_x^2 + g_y^2 + g_z^2) = g_L^2$) and that the ground state has its full 16-fold degeneracy. The suggestions by Blöte, Wielinga, and Huiskamp (ref. 11) and Townsend and Crossley (ref. 10) that the low-field magnetization results reported by van Geuns (ref. 2) for $Dy_2Ti_2O_7$ may have been plagued by just such a misinterpretation are substantiated by

the results reported here.

Returning to the discussion of the magnetic-entropy measurements, it is clear that once the isotherms in the S, H-plane have been properly located, it becomes a simple matter to plot the changes in magnetic entropy as a function of temperature for various constant values of applied magnetic field. A few of the isofield lines are shown in such a plot in figure 11. The data from figure 8 are shown by the dashed line. The points abcd outline one possible cycle for the ideal case when the entropy of the lattice has been ignored. In practice, however, the adiabatic legs of the cycle must be corrected for the entropy absorbed by the lattice. The resulting cycle required to achieve the same cooling capacity as the first cycle is outlined by the points aefd. The cooling capacity per gram of $Dy_2Ti_2O_7$ for this cycle is the amount of heat absorbed at 4.2 K given by

$$\Delta Q = T\Delta S = 0.031 \pm 0.004 \text{ J/g} \tag{10}$$

A refrigerator containing 1000 grams of $Dy_2Ti_2O_7$ and completing the indicated cycle once every minute will have, for example, a maximum cooling capacity of about 0.5 watt. Any actual refrigerator will, of course, have a capacity less than that because of the unavoidability of irreversible processes such as heat flow along temperature gradients and so on.

It should be pointed out that the absolute maximum cooling capacity for the compound studied in the present investigation, if used in a refrigeration cycle between 4.2 and 20 K, is just 0.047 joule per gram. The limitation is imposed by the maximum entropy change available at 20 K, with the sample assumed to have been adiabatically magnetized from zero magnetic field at 4.2 K. The resulting cycle is outlined by points aegh. The applied field required to aline the atomic magnetic moments completely at 20 K is well in excess of 10 tesla.

Lewis Research Center,
National Aeronautics and Space Administration,
Cleveland, Ohio, February 20, 1974,
502-10.

APPENDIX A

SYMBOLS

A	amplifier gain
a	specific-heat constant
C	capacitance
E	voltage proportional to heater power
E_i	integrator input voltage
E_m	multiplier output voltage
E_o	integrator output voltage
E_R	recorder input voltage
e	error voltage
g	spectroscopic filling factor
dH/dt	rate of change of magnetic field
H_{max}	maximum applied magnetic field
H_{min}	minimum applied magnetic field
I_H	heater current
J	total angular momentum quantum number
M	magnetization
M_S	saturation magnetization
N	number of magnetic ions per cm^3
n_B	number of Bohr magnetons per magnetic ion
Q	heat
$\dot{Q}$	heater power
R	universal gas constant
r	resistance
S	entropy
S_l	lattice entropy
S_m	magnetic entropy

T	absolute temperature
t	time
V_H	heater voltage
V_x, V_y	multiplier input voltages
Θ_D	Debye constant
μ_B	Bohr magneton

APPENDIX B

CALCULATION OF CORRECTION FACTOR

Figure 12 shows the variation of heater power required to maintain the sample at two representative temperatures as a function of applied magnetic field. The variation can be approximated reasonably well by a linear relation between heater power and field. Starting from this assumption, an analytical expression can be derived which can be used to correct the magnetic entropy data.

The multiplier output is given, for the particular instrument used, by

$$E_m = \frac{1}{10} V_x V_y \tag{B1}$$

where V_x and V_y are the input voltages. In this case, V_x is the voltage measured across a 100-ohm standard resistor in series with the heater and is

$$V_x = 100 I_H \tag{B2}$$

where I_H is the heater current. The amplified heater voltage V_y is given by

$$V_y = A V_H \tag{B3}$$

The quantity A represents an amplifier gain and is included because at times it was necessary to amplify the heater voltage to provide the multiplier with an acceptable input signal. Combining equations (B1) to (B3) gives

$$E_m = 10 A V_H I_H = 10 A \dot{Q} \tag{B4}$$

where $\dot{Q}$ is the power supplied to the heater. At $H = H_{max}$, the multiplier output is some constant value $E_{m,1}$. A bucking voltage equal to $E_{m,1}$ is supplied by an external source, so that the input to the integrator is zero. At $H = H_{min}$ the multiplier output is $E_{m,2}$, so that with the bucking voltage unchanged, an error voltage

$$e = E_{m,2} - E_{m,1} \tag{B5}$$

appears at the integrator input. At any intermediate field, the error voltage is given by

$$e = -\left(\frac{E_{m,2} - E_{m,1}}{H_{max} - H_{min}}\right)(H - H_{min}) + E_{m,2} - E_{m,1} = (E_{m,2} - E_{m,1})\left(1 - \frac{H - H_{min}}{H_{max} - H_{min}}\right) \tag{B6}$$

as discussed in the first paragraph in this appendix.

The integrator input voltage thus consists of two terms. The first is a multiplier output E_s, corresponding to the heater power required to keep the sample at a constant temperature as the magnetic field, and hence the magnetic entropy, is changed. The second is the error voltage. Thus, the total signal E_i to the integrator is

$$E_i = E_s + e = 10A\dot{Q}_s + e \tag{B7}$$

where $\dot{Q}_s$ is the rate at which heat is absorbed by the sample because of its changing magnetic entropy. The integrator output is given by

$$E_o = \frac{1}{rC}\int E_i \, dt \tag{B8}$$

where rC is the integrator time constant. Inserting equation (B7) into (B8) gives

$$E_o = \frac{1}{rC}\int (10A\dot{Q}_s + e)\, dt$$

$$= \frac{10A}{rC}\Delta Q_s + \frac{1}{rC}\int e \, dt \tag{B9}$$

Since the magnetic field may be considered to be a function of time, equation (B9) becomes

$$E_o = \frac{10A}{rC}\Delta Q_s + \frac{E_{m,2} - E_{m,1}}{rC}\int_{H_{max}}^{H}\left(1 - \frac{H - H_{min}}{H_{max} - H_{min}}\right)\left(\frac{dH}{dt}\right)^{-1} dH \tag{B10}$$

If dH/dt is kept constant over some range of field values, equation (B10) becomes

$$E_o = \frac{10A}{rC} \Delta Q_s + \frac{E_{m,2} - E_{m,1}}{rC\left(\frac{dH}{dt}\right)} \left[- \frac{1}{2} \frac{(H_{max} - H)^2}{H_{max} - H_{min}} \right] \tag{B11}$$

The integrator output can be divided by a factor proportional to T, so that the input to the recorder is actually

$$E_R = \frac{E_o}{T} = \frac{10A}{TrC} \Delta Q_s + \frac{E_{m,2} - E_{m,1}}{TrC\left(\frac{dH}{dt}\right)} \left[- \frac{1}{2} \frac{(H_{max} - H)^2}{H_{max} - H_{min}} \right] \tag{B12}$$

The change in magnetic entropy upon demagnetizating from H_{max} to H is finally given by

$$\Delta S_m = \frac{rCE_R}{10A} + \frac{E_{m,2} - E_{m,1}}{10TA\left(\frac{dH}{dt}\right)} \left[\frac{1}{2} \frac{(H_{max} - H)^2}{H_{max} - H_{min}} \right] \tag{B13}$$

REFERENCES

1. Brown, G. V.: The Practical Use of Magnetic Cooling. NASA TM X-52983, 1971.
2. van Geuns, J. R.: A Study of a New Magnetic Refrigeration Cycle. Thesis, Univ. of Leiden, 1966.
3. Roth, Robert W.: Pyrochlore-Type Compounds Containing Double Oxides of Trivalent and Tetravalent Ions. Jour. Res. Nat'l Bur. of Standards, vol. 56, no. 1, Jan. 1956, pp. 17-25.
4. Laurence, James C.: High-Field Electromagnets at NASA Lewis Research Center. NASA TN D-4910, 1968.
5. Lawless, W. N.: A Low Temperature Glass-Ceramic Capacitance Thermometer. Rev. Sci. Inst., vol. 42, no. 5, May 1971, pp. 561-566.
6. Rubin, L. G.; and Lawless, W. N.: Studies of a Glass-Ceramic Capacitance Thermometer in an Intense Magnetic Field at Low Temperature. Rev. Sci. Inst., vol. 42, no. 5, May 1971, pp. 571-573.
7. de Klerk, D.: Adiabatic Demagnetization. In Handbuch der Physik, vol. XV, S. Flugge, ed., Springer-Verlag (Berlin), 1956, pp. 38-209.
8. van Vleck, J. H.: The Theory of Electric and Magnetic Suspectibilities. Oxford Univ. Press, 1932.
9. Morrish, Allan H.: The Physical Principles of Magnetism. John Wiley & Sons, 1965.
10. Townsend, M. G.; and Crossley, W. A.: Magnetic Suspectibility of Rare-Earth Compounds with the Pyrochlore Structure. Jour. Phys. Chem. Solids, vol. 29, no. 4, 1968, pp. 593-598.
11. Blöte, H. W. J.; Wielinga, R. F.; and Huiskamp, W. J.: Heat-Capacity Measurements on Rare-Earth Double Oxides $R_2M_2O_7$. Physica, vol. 43, 1969, pp. 549-568.

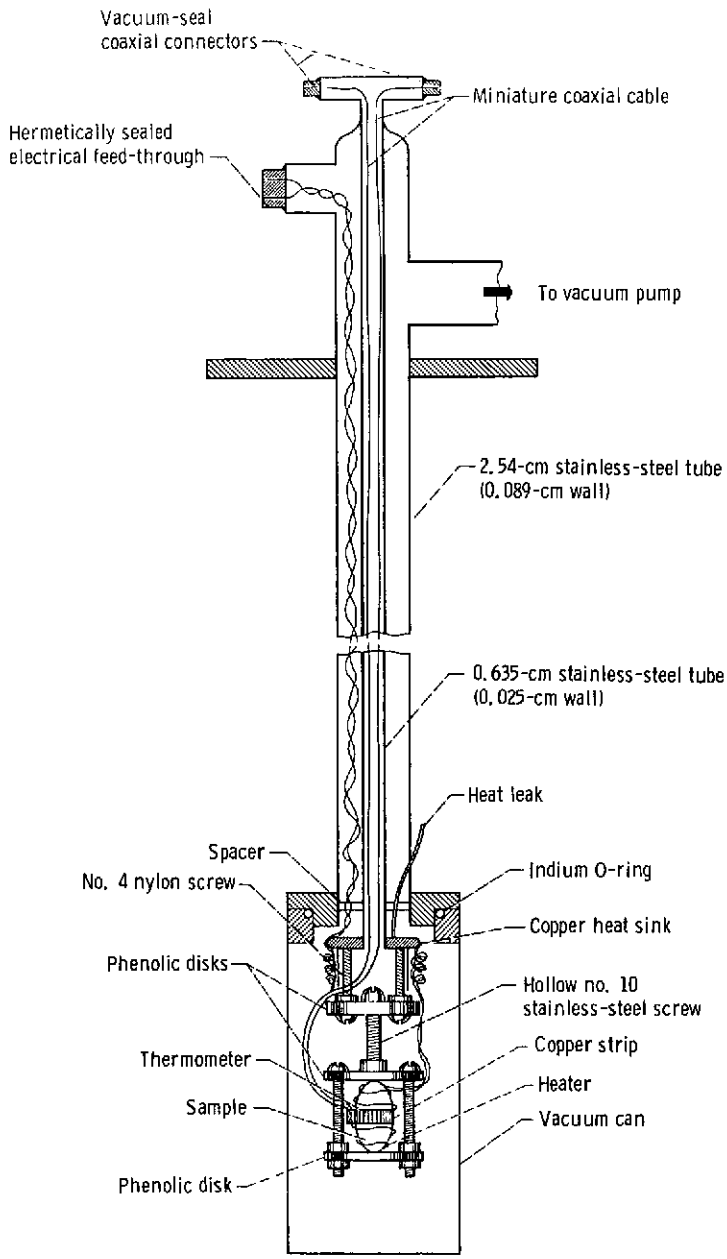

Figure 1. - Magnetic-entropy apparatus. (Not to scale.)

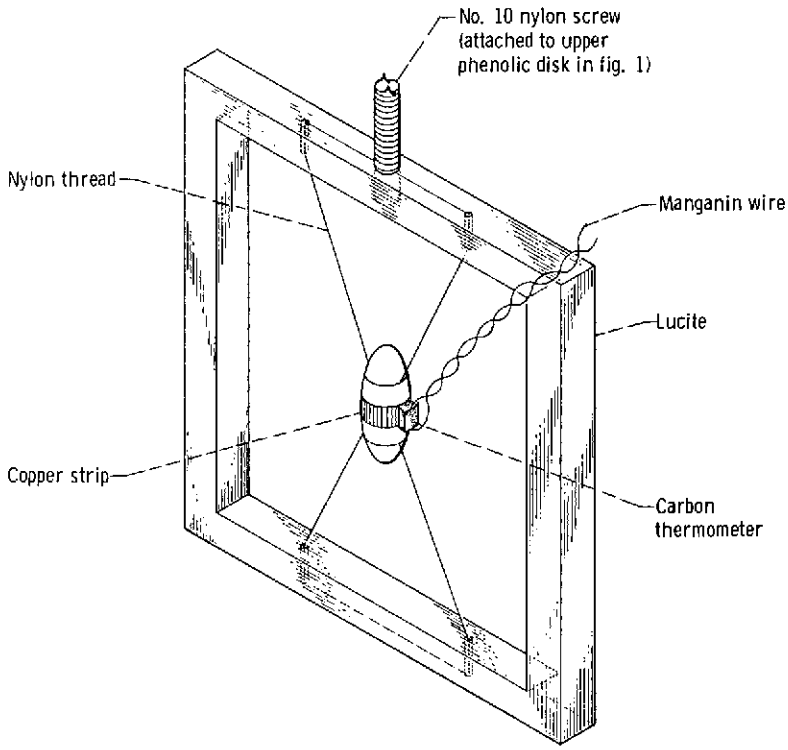

Figure 2. - Sample holder for adiabatic magnetization-demagnetization measurements. (Not to scale.)

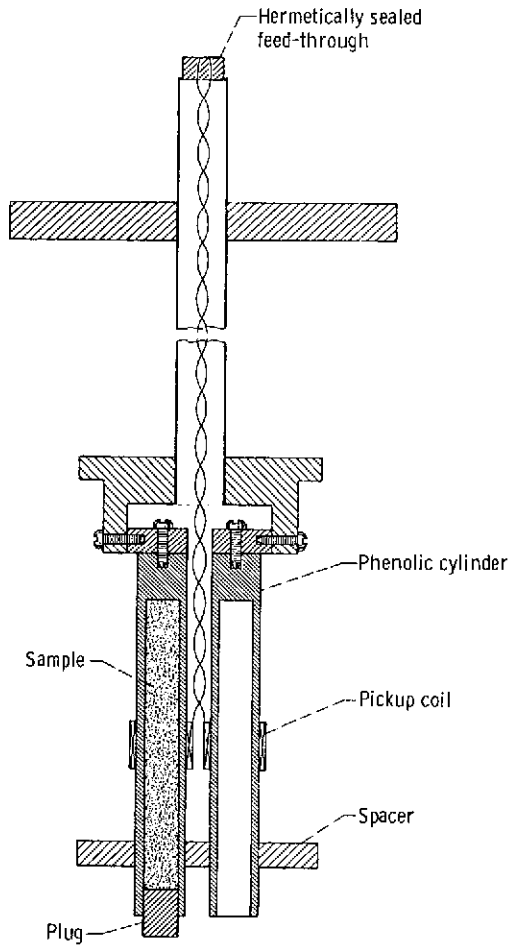

Figure 3. - Magnetization apparatus. (Not to scale.)

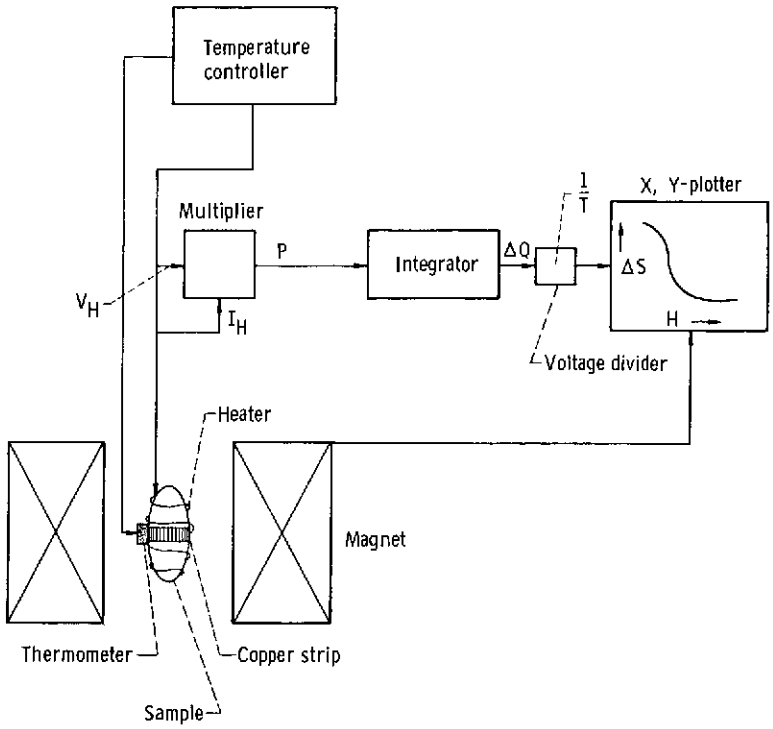

Figure 4. - Schematic diagram of magnetic-entropy measurement technique.

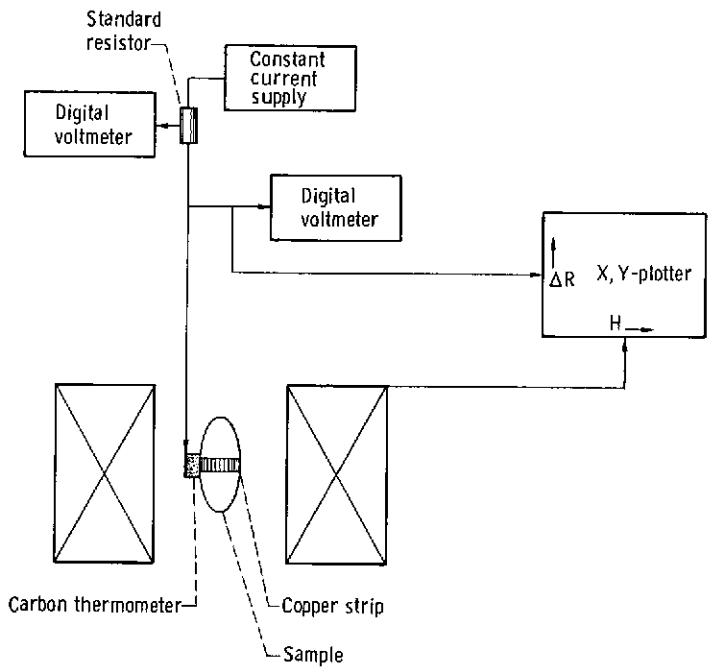

Figure 5. - Schematic diagram of measurement technique for adiabatic magnetization-demagnetization temperature changes.

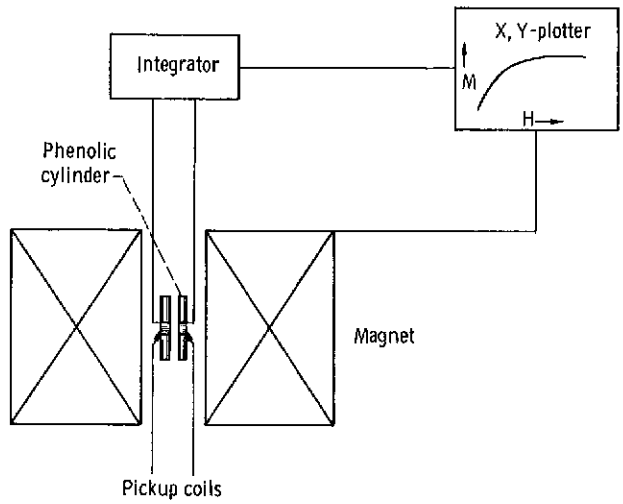

Figure 6. - Schematic diagram of magnetization measurement technique.

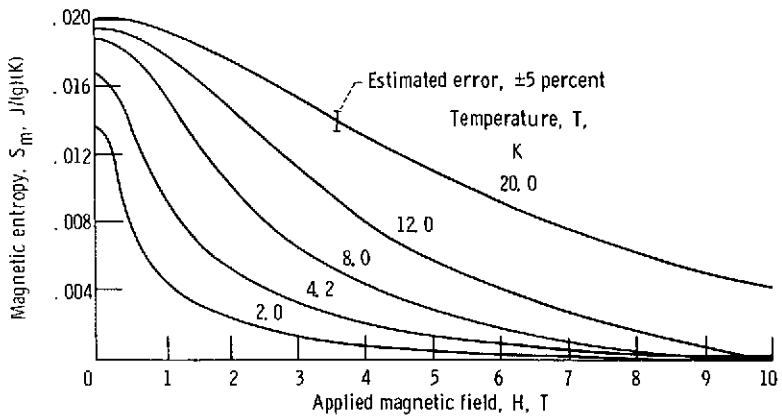

Figure 7. - Magnetic entropy as function of applied magnetic field.

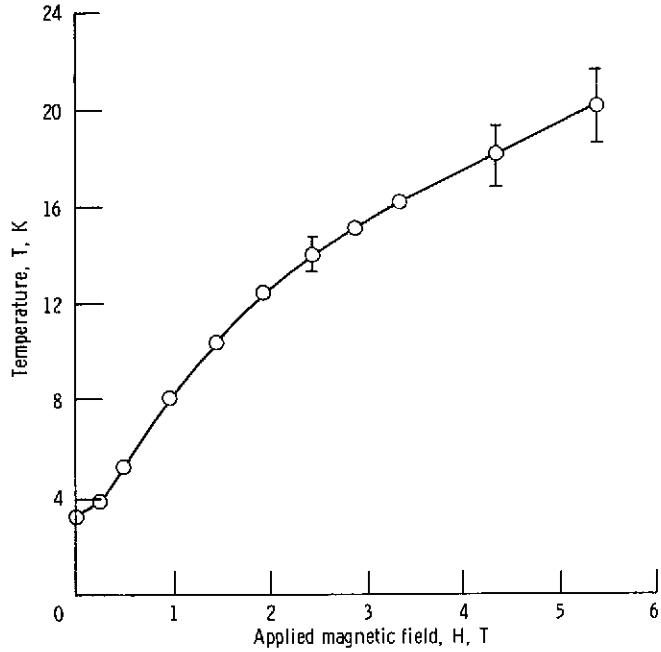

Figure 8. - Adiabatic magnetization of dysprosium titanium oxide.

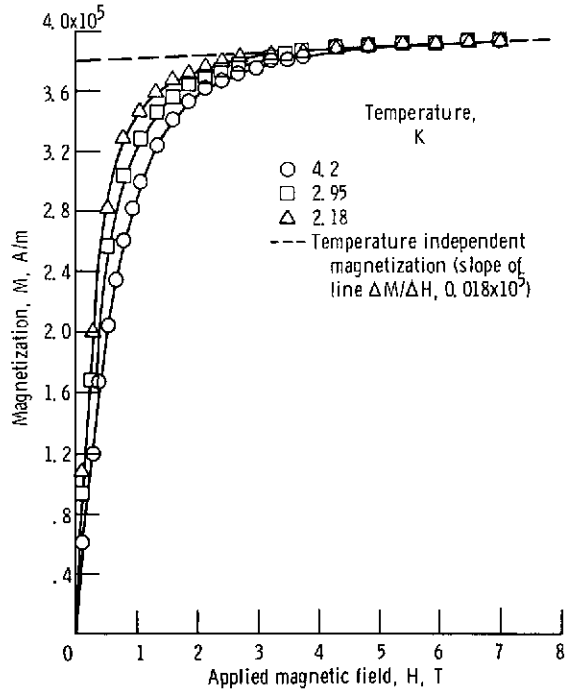

Figure 9. - Magnetization of dysprosium titanium oxide as function of applied magnetic field.

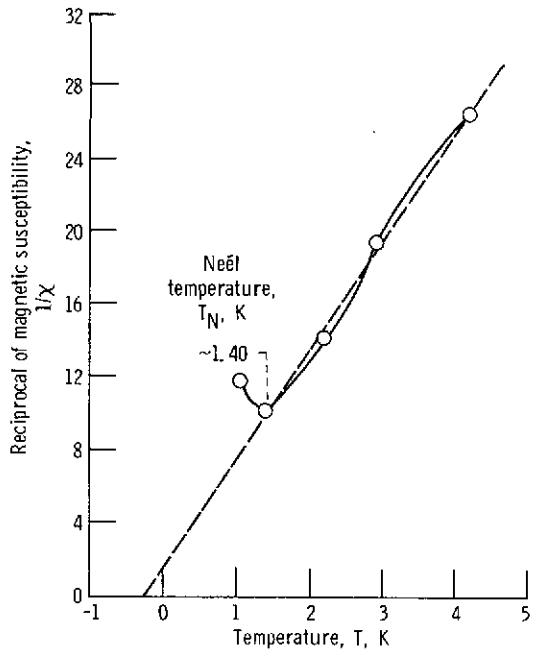

Figure 10. - Reciprocal magnetic susceptibility of dysprosium titanium oxide.

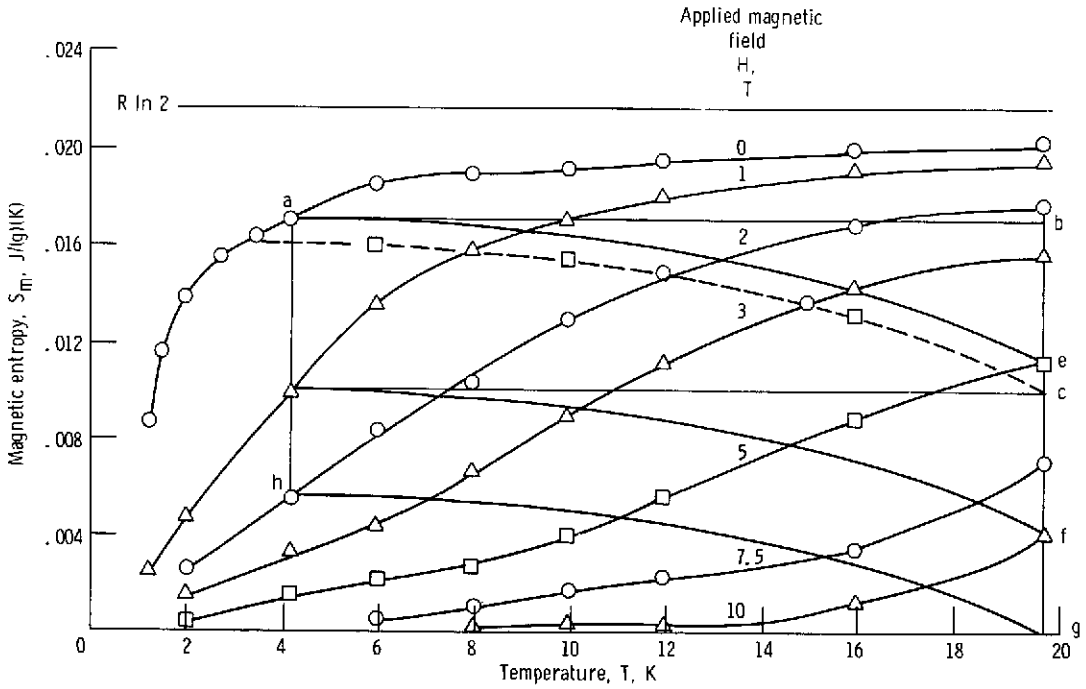

Figure 11. - Magnetic-entropy - temperature plane for dysprosium titanium oxide.

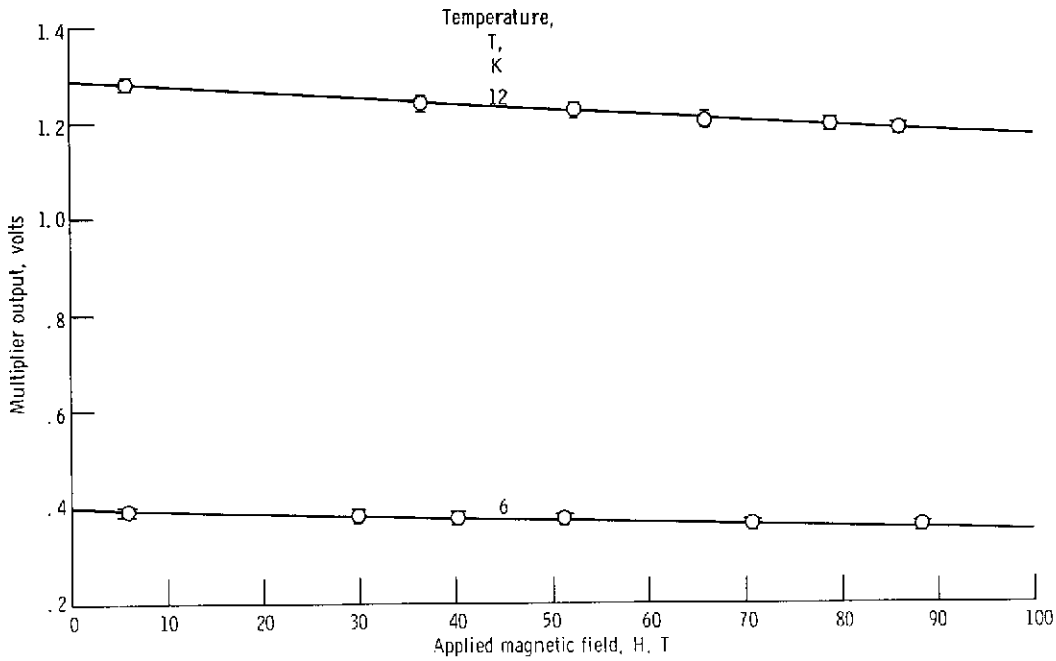

Figure 12. - Field dependence of heater power required to maintain isothermal conditions for typical runs.